Electronic Supplementary Material (ESI) for Chemical Science.

Engineering a bifunctional copper site in the cupredoxin fold

Andrés Espinoza-Cara[a,b], Ulises Zitare[c], Damián Alvarez-Paggi[c,d], Sebastián Klinke[d,e], Lisandro H. Otero[d,e], Daniel H. Murgida[c] and Alejandro J. Vila*[a,b,e]

Supplementary Methods

The reduction potential (E^0) values were determined by cyclic voltammetry (CV) of protein samples in solution, as the midpoint of the peak-to-peak separation: $E^0 = (E_{ap} + E_{cp})/2$, where E_{ap} and E_{cp} are the anodic and cathodic peak potencials, respectively. The electron transfer reorganization free energies (λ) were obtained from CV experiments performed on protein samples adsorbed on gold electrodes coated with biocompatible films. The films employed consist of a mixed self-assembled monolayer (SAM) of 60% of 1-mercapto-16-hexadecanol and 40% of 1-hexadecanethiol composition, to maximize the amount of adsorbed protein. The thickness of the SAM guarantees a low electronic coupling between the redox site and the electrode surface, yielding a tunneling-controlled electron transfer reaction. The rate constants of heterogeneous electron transfer at zero over-potential (k_{ET}^0) were determined from CVs acquired at variable scan rates (typically from 50 to 400 mV/s) using the Laviron's working curve[1]. This method evaluates the peak separation as a function of scan rate in CVs, for separations of the anodic and cathodic peaks of up to 200 mV. The working curve is valid for values of the charge transfer coefficient (α) of $0.3 < \alpha < 0.7$, which is suitable for the reported CVs considering the symmetric peaks of the voltammograms. The estimation of α value were performed by analyzing the width at half-height of both anodic (W_{ap}) and cathodic (W_{cp}) peaks of several voltammograms at different scan rates. Given both $W_{ap} = 62.5mV/n\alpha$ and $W_{cp} = 62.5mV/n(1-\alpha)$, therefore $\alpha = W_{ap}/(W_{ap} + W_{cp})$. The informed α values are the average obtained for both chimeras. k_{ET}^0 values were determined as a function of temperature between 5 and 39 °C. Under the usual approximation of negligibly small activation entropies, i.e. $\Delta G^* \approx \Delta H^* \approx \lambda/4$, we obtained λ directly from Arrhenius plots.

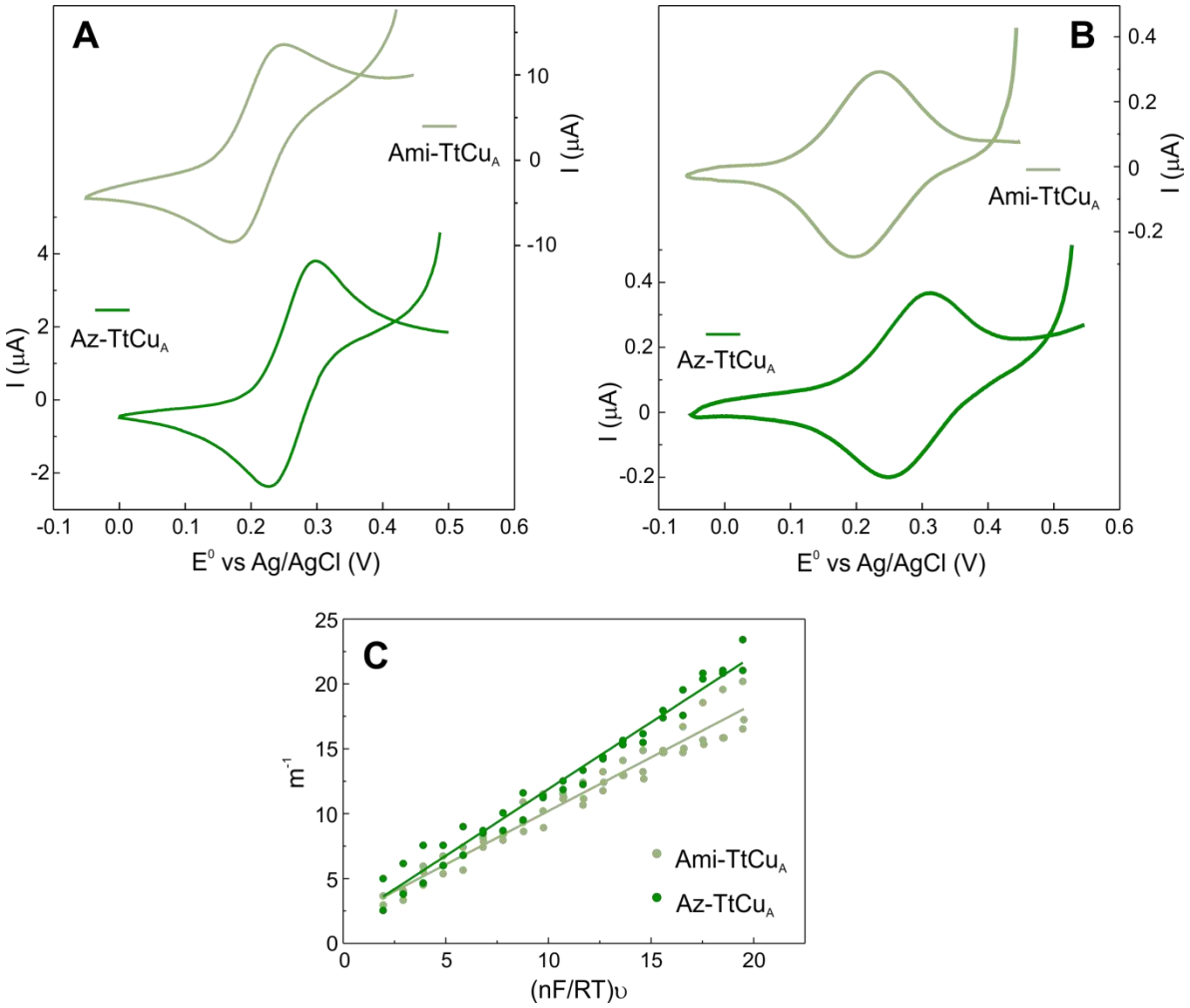

Supplementary Figure 1. A: Voltagrams of Ami-*Tt*Cu$_A$ (top, pale green) and Az-*Tt*Cu$_A$ (bottom, green) samples in solution, used to obtain the E^0 values reported. B: Voltagrams of Ami-*Tt*Cu$_A$ (top, pale green) and Az-*Tt*Cu$_A$ (bottom, green) adsorbed on SAM-coated gold electrodes, acquired at 25 °C at different scan rates from 50 to 500 mV/s, from which kinetic parameters were extracted. C: Laviron's working example curves obtained for determining k_{ET}^{o} values of Ami-*Tt*Cu$_A$ (pale green) and Az-*Tt*CuA (green) adsorbed on SAM-coated gold electrodes at 25°C.

Supplementary Table 1. Position of absorption bands from electronic spectroscopies in the chimeric proteins Ami-*Tt*Cu_A and Az-*Tt*Cu_A compared to other T1 sites.

		Az[1]	Pc[2]	PAz[3]	CBP[4]	*Ac*NiR[5]	Ami-*Tt*Cu_A	Az-*Tt*Cu_A
		Energy (cm^{-1})						
8	d_z^2	5,430	5,000	5,100	5,800	5,600	-	-
7	d_{xy}	10,700	10,800	10,400	10,800	11,900	10,600	10,700
6	d_{xz+yz}	12,600	12,800	12,500	12,900	13,500	12,200	12,400
5	d_{xz-yz}	13,700	13,950	13,500	14,100	14,900	14,100	14,400
4	Cys π	15,900	16,700	16,850	17,100	17,550	17,500	17,600
3	Cys σ	18,100	18,700	22,100	21,000	21,900	21,500	22,000
2	His σ	20,100	21,390	24,600	22,500	-	-	-
1	Met	21,900	23,440	18,700	24,750	25,650	25,000	25,100

Supplementary Table 2. EPR parameters of Ami-*Tt*Cu_A and Az-*Tt*Cu_A and their imidazole adducts compared to other T1 copper proteins

Parameter	Ami[2,3]	Az[2,3]	Paz[4]	Pc[5]	CBP[4,6]	*Ac*NiR[7]	*Rs*NiR[7]	Ami-*Tt*Cu_A	Ami-*Tt*Cu_A + Im^-	Az-*Tt*Cu_A	Az-*Tt*Cu_A + Im^-	Nc[8–10]
EPR	ax	ax	rh	ax	rh	rh		rh	ax	rh	ax	ax
g_x	2.032	2.035	2.015	2.035	2.018	2.02	-	2.019	2.036	2.031	2.041	2.036
g_y	2.047	2.054	2.053	2.044	2.059	2.06	-	2.066	2.058	2.059	2.053	2.059
g_z	2.235	2.261	2.213	2.233	2.205	2.19	2.19	2.195	2.233	2.198	2.228	2.245
A_x [mT]	0.6	1.4	7.3	0.5	-	-	-	2.5	0.7	3.1	1.2	-
A_y [mT]	0.8	1.4	1.8	0.8	-	-	-	0.4	0.8	0.7	1.1	2.5
A_z [mT]	5.4	5.3	3.5	6.0	5.6	7.13	7.13	8.8	12.8	8.4	13.8	13.8

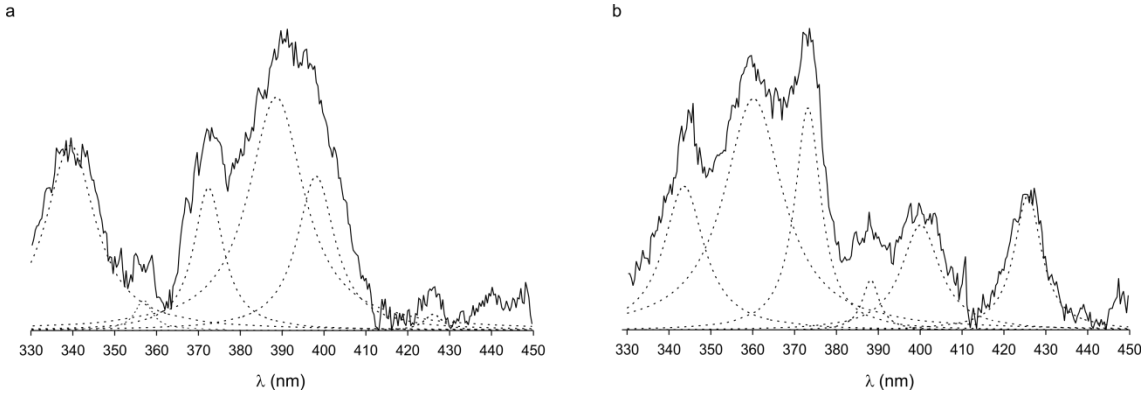

Supplementary Figure 2. Resonance Raman spectra acquired with 633 nm excitation at pH 7 for Ami-*Tt*Cu_A (a) and Az-*Tt*Cu_A (b). Lorentzian component bands are shown as black dotted lines, and the corresponding parameters are specified in Supplementary Table 2.

Supplementary Table 3. Lorentzian position and Intensities from the Resonance Raman Spectra of Ami-*Tt*Cu_A and Az-*Tt*Cu_A used for the calculation of the Effective Stretching Vibrational Frequency.

Ami-*Tt*Cu_A		Az-*Tt*Cu_A	
ν_i (cm^{-1})	I (a.u.)	ν_i (cm^{-1})	I (a.u.)
339.5	0.61	343.6	0.47
372.4	0.47	360.2	0.77
388.6	0.77	373.2	0.73
398.1	0.51	388.2	0.16
426.1	0.09	400.1	0.34
-	-	425.7	0.45

Supplementary Table 4. Effective Stretching Vibrational Frequency $\langle \nu_{Cu-S_{Cys}} \rangle$ for different T1 proteins.

Protein	$\langle \nu_{Cu-S_{Cys}} \rangle$, cm^{-1}
Az	407
Ami	406
Pc	403
Paz	396
CBP	394
AcNiR	383
Ami-*Tt*Cu_A	379
Az-*Tt*Cu_A	378

Supplementary Table 5. Hyperfine-Shifted ^{1}H NMR Signals corresponding to Copper Ligands in Ami-*Tt*Cu$_A$ and Az-*Tt*Cu$_A$ recorded at 600 MHz in 100 mM KPi + 100 KCl at pD* 7.0 in D_2O. Values are indicated in ppm.

	Ami-*Tt*Cu$_A$ (298 K)	**Ami-*Tt*Cu$_A$ (310 K)**	**Az-*Tt*Cu$_A$ (298 K)**
A	56.1	53.8	55.0
B	51.5	48.5	38.0
C	42.7	41.5	30.0
D	26.8	25.8	24.0
E	23.5	23.4	
F	24.0	-	
G	-13.7	-12.6	

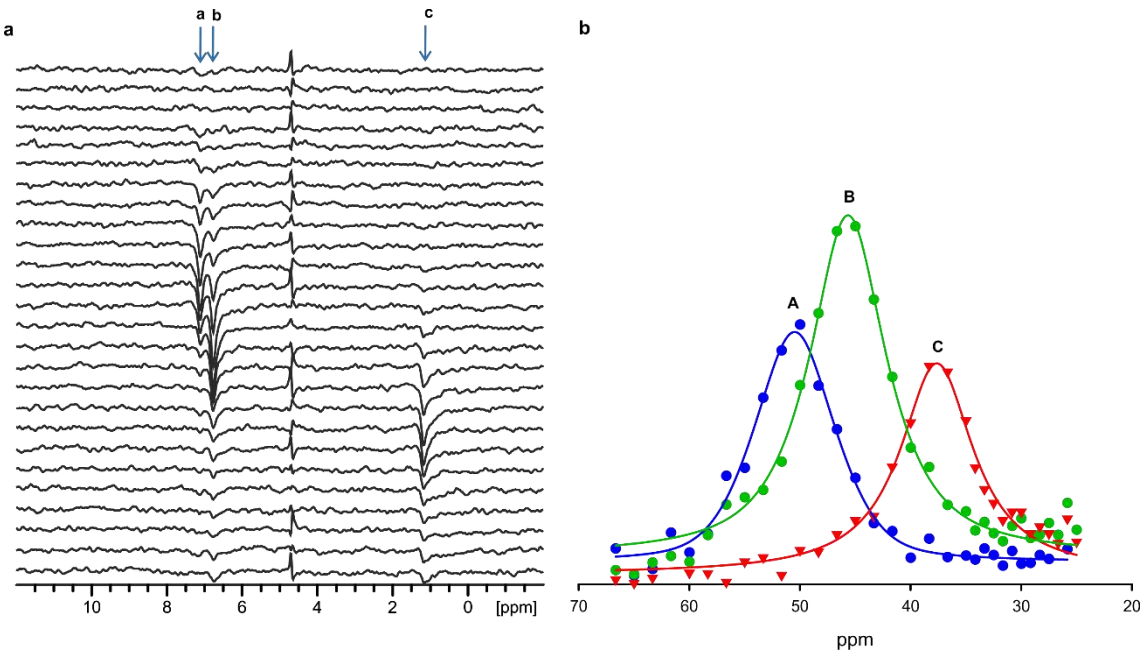

Supplementary Figure 3. (a) Saturation transfer ^{1}H NMR (600 MHz) experiment of Ami-*Tt*Cu$_A$ in 100 mM KPi + 100 KCl at pD* 7.0 in D_2O at 310 K obtained by irradiation at different frequencies. (b) Reconstructed ^{1}H NMR spectrum of Ami-*Tt*Cu$_A$ obtained by plotting the intensity of the exchange responses in the saturation transfer experiment as a function of the decoupler irradiation frequency, and by fitting these values to a modified Gaussian function (indicated as a continuous line in the plot).

Supplementary Table 6. Assigned Hyperfine Shifted Resonances in the ^{1}H NMR Spectra of T1 Cupredoxins compared with those from Az-*Tt*Cu$_A$ and Ami-*Tt*Cu$_A$

δ_{obs} (ppm)											
	***Pv*Ami**	***Pv*Ami**	**Az**	**Pc**	**CBP**	***Ac*NiR**	***Ax*NiR**	***Ac*PAz**	**Rc**	**Ami-*Tt*Cu$_A$**	**Az-*Tt*Cu$_A$**
HisB $C^{\delta 2}H$	43	43	49.1	47.1	50	45	44	46.1	50.2	45.2 (B)	-
HisA $C^{\delta 2}H$	50	50	54.0	51.6	60	58	54	53.5	58.1	50.0 (A)	-
HisB $C^{\epsilon 1}H$	-	35	46.7/34.1	35.6	-	-	33	32.0	36.7	-	-
HisA $C^{\epsilon 1}H$	-				-	-	-		30.3	-	-
Met $C^{\gamma 2}H$	12/11.1	12/11.1	-	23.5	-	-	-	-	-	-	-
Met $C^{\gamma 1}H$			-	13.0	32	25.1	<18	-	-	-	-
HisB $N^{\epsilon 2}H$	27.5	27.5	26.9	31.4	23.7	22.7	-	23	25.3	24 (F)	24 (C)
HisA $N^{\epsilon 2}H$	-	-	27	-	-	-	-	-	-	-	-
Asn/Ser/Gly $C^{\alpha}H$	-	14.1	19.9	17	17.2	15.3	16.3	17.4	19.5	-	-
Met $C^{\epsilon}H$	-	-	-	-	-	-	-	12.1	8.1	37.7 (C)	-
Cys $C^{\alpha}H$	14.1	-9.5	-7.0	-8.0	-8.7	-10.8	-	-	-	-	-
NH Asn	-	-	-30	-19	-	-	-	-15	-20	-	-
HisB $C^{\beta 2}H$	-9.5	-	-	-	-	-	-	-	-	-	-
HisB $C^{\beta 3}H$	-2.5	-	-	-	-	-	-	-	-	-	-

Diamagnetic assignments are not available for Az-*Tt*Cu$_A$ and Ami-*Tt*Cu$_A$, we have used the chemical shifts observed in the reduced proteins, as compared to typical values for Type 1 copper proteins, for assignment of the Az-*Tt*Cu$_A$ and Ami-*Tt*Cu$_A$ signals. Saturation transfer experiments of Az-*Tt*Cu$_A$ gave off-resonance responses so it was not possibly to assign resonance other than the exchangeable proton of the histidine.

Conditions of the experiments for the other Type 1 copper proteins listed in the table:

Paraccocus versutus Amicyanin (*Pv*Ami): 600 MHz, 305 K, 99% D_2O, ~6 mM, 50 mM phosphate buffer pH 7.0.[11] *Paraccocus versutus* Amicyanin (*Pv*Ami): 600 MHz, 305 K, 99% D_2O, ~6 mM, 50 mM phosphate buffer pH 7.0. [2] Azurin(Az): 800 MHz, 298 K, 99% D_2O, ~5 mM, 10 mM phosphate buffer pH 8.0.[12] Spinach Plastocyanin (Pc): 800 MHz, 298 K, 99% D_2O, ~3 mM, 50 mM phosphate buffer pH 7.5.[13] Cucumber Basic Protein (CBP): 500 MHz, 298 K, 99% D_2O, ~5 mM, 10 mM phosphate buffer pH 8.0.[6] *Achromobacter cycloclastes* Nitrite Reductase (*Ac*NiR): 500 MHz, 298 K, 99% D_2O, ~2 - 3 mM, 20 mM phosphate buffer pH 7.5.[14] *Achromobacter xylosoxidans* Nitrite Reductase (*Ax*NiR): 500 MHz, 298 K, 99% D_2O, ~2 - 3 mM, 20 mM phosphate buffer pH 7.5.[14] *Achromobacter cycloclastes* Pseudoazurin(*Ac*PAz): 800 MHz, 298 K, 99% D_2O, ~ 2 - 5 mM, 100 mM Tris-HCl buffer pH 8.0.[15] Rusticyanin (Rc): 800 MHz, 296 K, 99% D_2O, ~ 2 - 5 mM, 100 mM acetate buffer pH 5.5.[15]

Supplementary Table 7. Crystallographic data collection and refinement statistics

Data collection		
Number of frames		395
Oscillation step (deg)		0.5
Detector distance (mm)		55
Wavelength (Å)		1.5418
Exposure per frame (s)		75
Indexing and scaling		
Cell parameters	a (Å)	94.35
	b (Å)	100.70
	c (Å)	101.10
	α = β = γ (deg)	90
Space group		$P2_12_12_1$
Resolution limit (Å)		2.30
Number of total reflections		334728
Number of unique reflections		42870
Average multiplicity [a]		7.8 (7.6)
$\langle I/\sigma(I) \rangle$		12.2 (2.2)
R_{meas}		0.154 (0.999)
R_{pim}		0.054 (0.360)
$CC_{1/2}$		0.997 (0.751)
Completeness (%)		99.8 (97.5)
No. of chains per asymmetric unit		8
Solvent content (%)		47
Overall B-factor (Wilson plot, Å^2)		35
Refinement		
Resolution range (Å)		45.18-2.30
Number of protein atoms		7164
Number of ligand atoms		24
Number of water molecules		541
R		0.178
R_{free}		0.226
Rms deviations from ideal values[24]		
Bond lengths (Å)		0.010
Bond angles (deg)		1.1
Average B-factor (Å^2)		
Protein		34
Ligand		42
Water		40
MolProbity validation[9]		
Clashscore		4.71
MolProbity score		1.91
Ramachandran plot		
Favored (%)		97.4
Allowed (%)		2.6
Disallowed (%)		-
Deposition		
PDB code		5U7N

[a] Values in parentheses correspond to the highest resolution shell (2.38-2.30 Å)

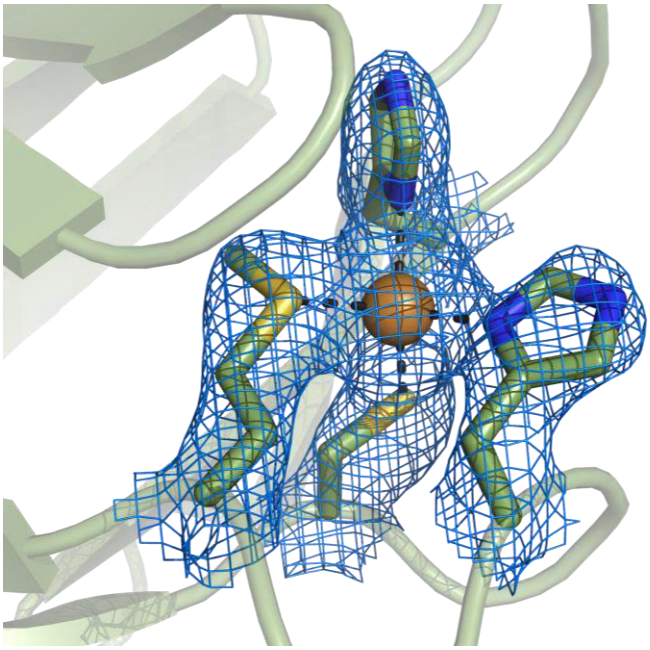

Supplementary Figure 4. Model of the Cu(II) site of Ami-*Tt*Cu_A the 2Fo-Fc (contoured at 1.3 σ, blue) electron densities. The ligands and the mutated residues on the loop are labeled.

Supplementary Table 8. Copper-Ligand distances for Ami-*Tt*Cu_A in each monomer from the crystal structure and their average.

	S_{Cys}^{149}-Cu	S_{Met}^{155}-Cu	N_{His}^{152}-Cu	N_{His}^{114}-Cu
a	2.36	2.33	2.01	2.23
b	2.51	2.43	1.98	2.21
c	2.40	2.38	1.97	2.17
d	2.42	2.34	1.91	2.16
e	2.27	2.33	2.04	2.26
f	2.44	2.28	2.00	2.17
g	2.49	2.37	2.08	2.13
h	2.37	2.37	1.96	2.19
Average	**2.41 ± 0.07**	**2.35 ± 0.04**	**1.99 ± 0.05**	**2.19 ± 0.04**

Supplementary Table 9. Ligand-Copper-Ligand angles for Ami-*Tt*Cu_A in each monomer from the crystal structure and their average.

	S^{149}-Cu-N^{152}	**S^{149}-Cu-N^{114}**	**N^{152}-Cu-N^{114}**	**S^{149}-Cu-S^{155}**	**N^{152}-Cu-S^{155}**	**N^{114}-Cu-S^{155}**
a	101.4	127.5	97.3	114.4	122.8	94.6
b	97.2	128.2	99.3	116.0	123.0	94.6
c	100.1	133.6	101.8	108.7	121.4	93.7
d	99.4	127.2	103.3	112.9	123.7	92.5
e	104.3	130.4	92.9	120.0	117.4	90.0
f	97.7	127.4	100.9	114.4	127.6	91.5
g	93.8	132.4	104.6	113.5	120.6	94.3
h	99.6	129.1	101.9	112.0	124.6	92.3
Average	**99.2 ± 3.1**	**129.5 ± 2.4**	**100.24 ± 3.7**	**114.0 ± 3.3**	**122.63 ± 3.0**	**92.92 ± 1.7**

Supplementary Table 10. Ami- *Tt*Cu_A Cu-Ligand distances and L-Cu-L Angles compared to other T1 copper proteins

	Ami-*Tt*Cu_A (5U7N)	Ami (1AAC)	Pc (1PLC)	CBP (1CBP)	NiR (1NIF)
Distances (Å)					
S^{γ}_{Cys}-Cu	2.41	2.11	2.07	2.16	2.16
S^{δ}_{Met}-Cu	2.35	2.87	2.82	2.61	2.55
$N^{\delta1}_{HisL9}$-Cu	1.99	2.03	2.06	1.95	2.00
$N^{\delta1}_{HisL5}$-Cu	2.19	1.95	1.91	1.93	2.06
Angles					
$N^{\delta1}_{HisL5}$-Cu-$N^{\delta1}_{HisL9}$	100.9	104.0	97.2	99.3	97.0
$N^{\delta1}_{HisL5}$-Cu-S^{δ}_{Met}	91.5	84.5	88.5	83.0	86.6
$N^{\delta1}_{HisL5}$-Cu-S^{γ}_{Cys}	127.4	136.4	131.7	138.1	136.5
$N^{\delta1}_{HisL9}$-Cu-S^{δ}_{Met}	127.6	100.3	100.6	112.1	131.7
$N^{\delta1}_{HisL9}$-Cu-S^{γ}_{Cys}	97.7	112.5	121.0	110.4	104.2
S^{γ}_{Cys}-Cu-S^{δ}_{Met}	114.4	110.5	109.0	110.6	105.5
The subscript His_{L9} to the metal binding loop histidine $C(X)_nH(X)_mM$ while the subscript His_{LS} refers to the histidine in the surrounding loop.					

Supplementary Table 11. Hydrogen-Bonds Distances (in Å) in Ami-*Tt*Cu_A compared to the parent proteins.

Ami-*Tt*Cu_A (5U7N)		**Ami (1AAC)**		***Tt*Cu_A (2CUA)**	
$N_{Met155} \leftrightarrow O_{His152}$	3.08	$N_{Met98} \leftrightarrow O_{His95}$	2.90	$N_{Met160} \leftrightarrow O_{His157}$	3.16
$O_{Met155} \leftrightarrow N_{Cys149}$	3.55	$N_{Cys92} \leftrightarrow O_{Met98}$	3.17	$N_{Cys149} \leftrightarrow O_{Met160}$	3.50
$S^{\gamma}_{Cys149} \leftrightarrow N_{Gly115}$	3.25	$S^{\gamma}_{Cys92} \leftrightarrow N_{Asn54}$	3.64	$S^{\gamma}_{Cys149} \leftrightarrow N_{Gly115}$	3.50
$S^{\gamma}_{Cys149} \leftrightarrow N_{His152}$	3.75	$S^{\gamma}_{Cys92} \leftrightarrow N_{His95}$	4.04		
$O_{Cys149} \leftrightarrow N_{His152}$	3.46	$O_{Cys92} \leftrightarrow N_{His95}$	3.07		
$N^{\varepsilon 2}_{His114} \leftrightarrow O^{\delta 1}_{Asp111}$	2.80	$N^{\varepsilon 2}_{His53} \leftrightarrow O^{\varepsilon 2}_{Glu49}$	2.74	$N^{\varepsilon 2}_{His114} \leftrightarrow O^{\delta 1}_{Asp111}$	2.84
$O^{\delta 1}_{Asp111} \leftrightarrow N_{Val112}$	2.69	-	-	$O^{\delta 1}_{Asp111} \leftrightarrow N_{Val112}$	2.52
$OH_{Tyr90} \leftrightarrow O_{Gly115}$	2.64	$OH_{Tyr30} \leftrightarrow O_{Asn54}$	2.77	$OH_{Tyr90} \leftrightarrow O_{Gly115}$	2.63
-	-	$N_{Thr93} \leftrightarrow O^{\delta 1}_{Asn54}$	2.82	-	-
-	-	$O^{\gamma 1}_{Thr93} \leftrightarrow N^{\delta 2}_{Ans54}$	2.90	-	-
-	-	$O^{\gamma 1}_{Thr93} \leftrightarrow N^{\delta 1}_{His56}$	2.72	-	-
-	-	$O_{Pro96} \leftrightarrow N^{\eta}H_{2Arg99}$	3.20	-	-
-	-	$O_{Pro96} \leftrightarrow N^{\varepsilon 1}_{Arg99}$	2.71	-	-
$O_{His152} \leftrightarrow N_{Phe154}$	3.11	$O_{His95} \leftrightarrow N_{Phe97}$	3.01	-	-
$O_{Phe154} \leftrightarrow N_{Phe156}$	3.76	$O_{Phe97} \leftrightarrow N_{Arg99}$	3.45	$O_{Asn159} \leftrightarrow N_{Phe161}$	3.29

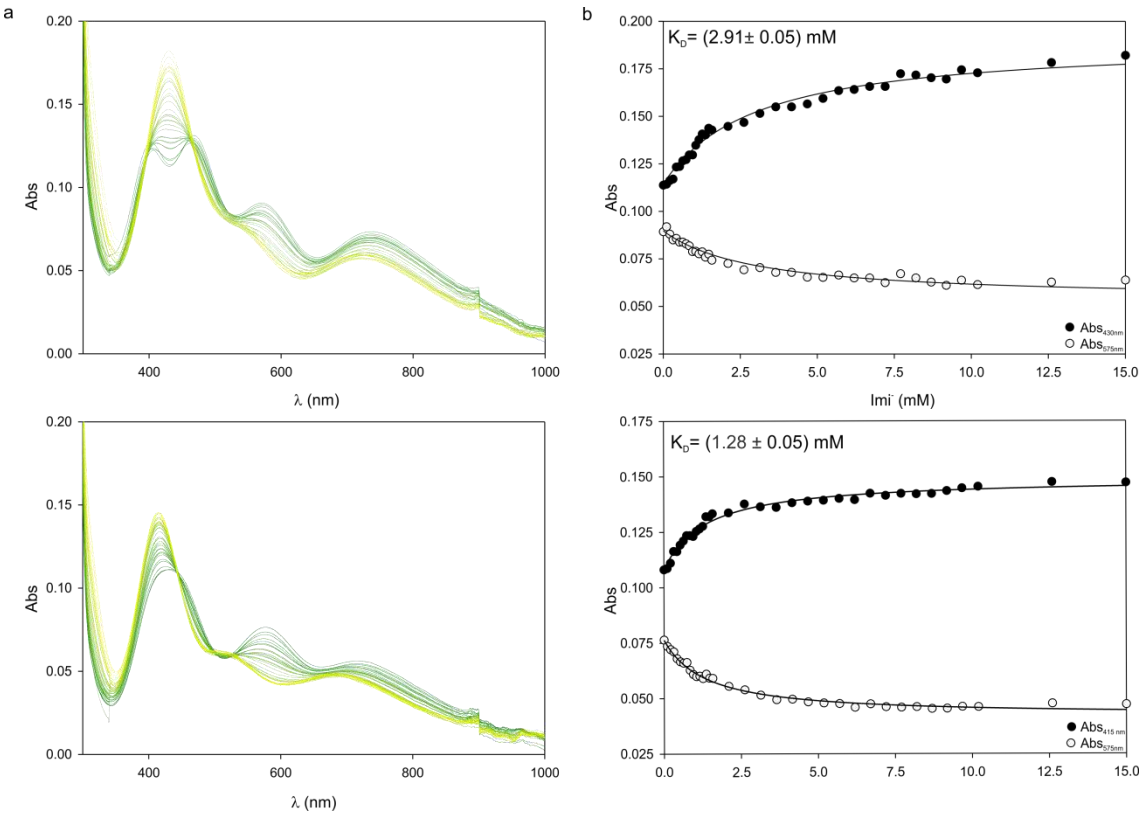

Supplementary Figure 5. a) Electronic Spectra of Ami-*Tt*Cu$_A$ (upper panel) and Az-*Tt*Cu$_A$ (lower panel) recorded upon increasing concentrations of imidazole. The titration progresses from green to yellow spectra. The spectra were obtained on Tris (100 mM) and NaCl (100 mM) pH 7.0 at 298 K. b) Evolution of the absorbances of Ami-*Tt*Cu$_A$ (upper panel) and Az-*Tt*Cu$_A$ (lower panel) as function of the total imidazole anion concentration. The wavelengths used where the ones that showed the highest changes in absorption and are shown as insets. The results of the fits to the binding model are shown as lines overlaid with the experimental data (dots). The K_d parameters derived from the fit with the program DynaFit where 2.91 ± 0.05 mM for Ami-*Tt*Cu$_A$ and 1.28 ± 0.05 mM for Az-*Tt*Cu$_A$.

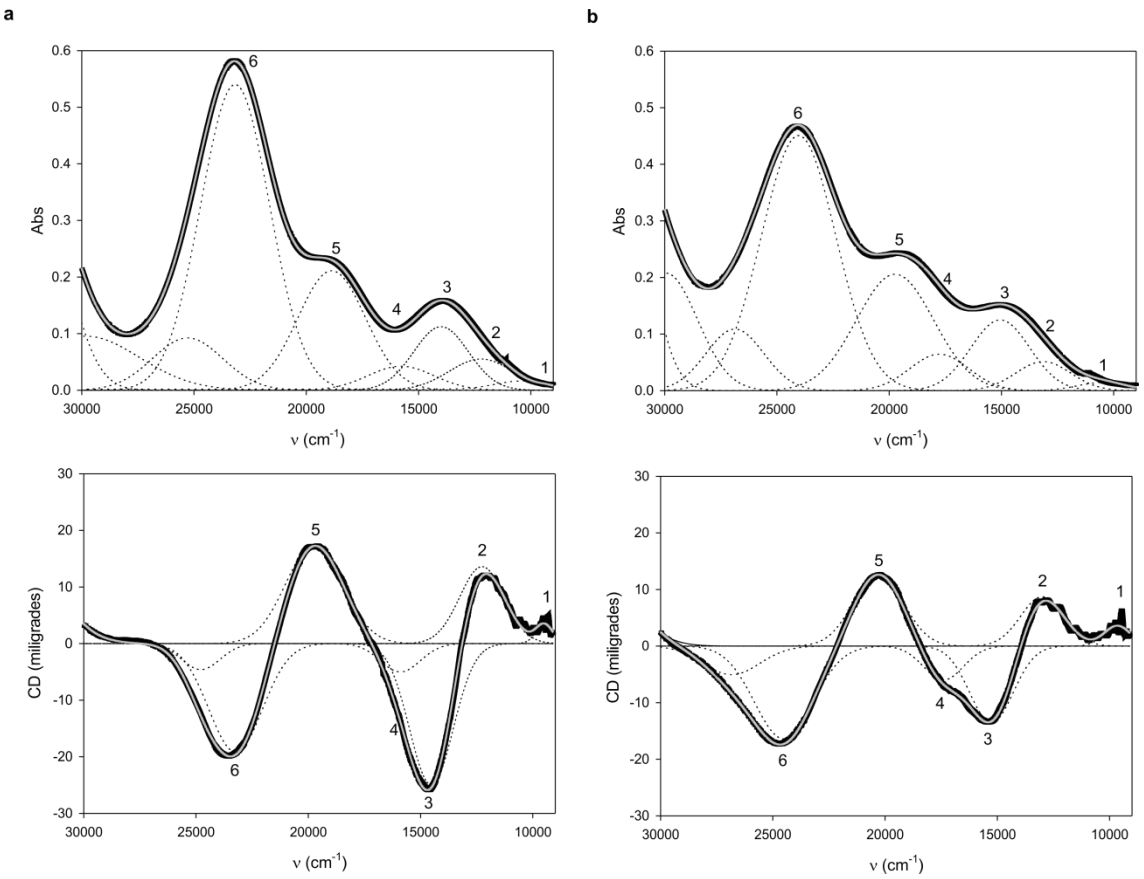

Supplementary Figure 6. Electronic Spectra of Imidazole Adducts. a) Electronic absorption (upper panel), circular dichroism spectra (lower panel) of Ami-*Tt*Cu_A. b) Electronic absorption (upper panel) and circular dichroism spectra (lower panel) of Az-*Tt*Cu_A. The spectra were obtained on Tris (100 mM) and NaCl (100 mM) and excess of Imidazole (50 mM) pH 7.0 at 298 K. Gaussian resolution of bands in the absorption spectra is based on a simultaneous linear least-squares fit of the absorption and CD data for each protein adduct, the simulated spectra are shown in gray. The bands have been labeled 1-6 for both proteins adducts; the numbering scheme is chosen to be consistent with the assignment of bands in nitrosocyanin. Bands to higher energy than band 6 in the spectra are necessary but are not labeled as they have no numbered counterpart in nitrosocyanin.

Supplementary Table 12. Position of absorption bands from electronic spectroscopies in the imidazole adducts of the chimeric proteins Ami-*Tt*Cu_A and Az-*Tt*Cu_A compared to nitrosocyanin.

		Nitrosocyanin[10]	Ami-*Tt*Cu_A –Imidazole	Az-*Tt*Cu_A - Imidazole
		Energy (cm^{-1})		
1	d_{xz}	10,500	9,300	-
2	d_{yz}	12,900	12,000	12,900
3	d_z^2	15,000	14,000	15,000
4	d_{xy}	17,600	15,500	17,500
5	Cys π	20,350	18,850	19,500
6	Cys σ	25,550	23,150	23,800

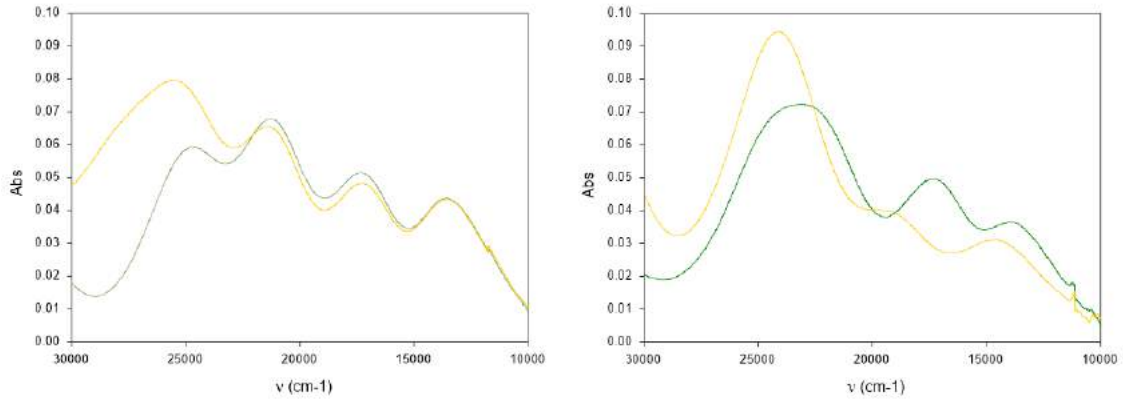

Supplementary Figure 7. Electronic Absorption Spectra of the Azide Adducts of Ami-*Tt*Cu_A(left) and Az-*Tt*Cu_A(right). Spectra wild of the resting state protein are shown in green, and spectra recorded upon addition of 50 mM of sodium azide are shown in yellow. The spectra were obtained on 100mM Tris-HCl, 100 mM NaCl at pH 7.0 and 298 K.

Bibliography

(1) Laviron, E. *J. Electroanal. Chem. Interfacial Electrochem.* **1979**, *101*, 19–28.

(2) Yanagisawa, S.; Dennison, C. *J Am Chem Soc* **2004**, *126*, 15711–15719.

(3) Li, C.; Yanagisawa, S.; Martins, B. M.; Messerschmidt, A.; Banfield, M. J.; Dennison, C. *Proc Natl Acad Sci U S A* **2006**, *103*, 7258–7263.

(4) Harrison, M. D.; Yanagisawa, S.; Dennison, C. *Biochemistry* **2005**, *44*, 3056–3064.

(5) Li, C.; Banfield, M. J.; Dennison, C. *J Am Chem Soc* **2007**, *129*, 709–718.

(6) Yanagisawa, S.; Dennison, C. *J Am Chem Soc* **2005**, *127*, 16453–16459.

(7) Solomon, E. I.; Szilagyi, R. K.; DeBeer George, S.; Basumallick, L. *Chem Rev* **2004**, *104*, 419–458.

(8) Arciero, D. M.; Pierce, B. S.; Hendrich, M. P.; Hooper, A. B. *Biochemistry* **2002**, *41*, 1703–1709.

(9) Berry, S. M.; Bladholm, E. L.; Mostad, E. J.; Schenewerk, A. R. *J Biol Inorg Chem* **2011**, *16*, 473–480.

(10) Basumallick, L.; Sarangi, R.; DeBeer George, S.; Elmore, B.; Hooper, A. B.; Hedman, B.; Hodgson, K. O.; Solomon, E. I. *J Am Chem Soc* **2005**, *127*, 3531–3544.

(11) Kalverda, A. P.; Salgado, J.; Dennison, C.; Canters, G. W. *Biochemistry* **1996**, *35*, 3085–3092.

(12) Bertini, I.; Fernández, C. O.; Karlsson, B. G.; Leckner, J.; Luchinat, C.; Malmström, B. G.; Nersissian, A. M.; Pierattelli, R.; Shipp, E.; Valentine, J. S.; Vila, A. J. *J Am Chem Soc* **2000**, *122*, 3701–3707.

(13) Bertini, I.; Ciurli, S.; Dikiy, A.; Gasanov, R.; Luchinat, C.; Martini, G.; Safarov, N. *J Am Chem Soc* **1999**, *121*, 2037–2046.

(14) Dennison, C.; Oda, K.; Kohzuma, T. *Chem. Commun.* **2000**, 751–752.

(15) Donaire, A.; Jiménez, B.; Fernández, C. O.; Pierattelli, R.; Niizeki, T.; Moratal, J.-M.; Hall, J. F.; Kohzuma, T.; Hasnain, S. S.; Vila, A. J. *J Am Chem Soc* **2002**, *124*, 13698–13708.

(16) Engh, R. A.; Huber, R. *Acta Crystallogr A Found Crystallogr* **1991**, *47*, 392–400.